Spectral Methods Based on Prolate Spheroidal Wave Functions for Hyperbolic PDEs *

Qianyong Chen[†], David Gottlieb[†], Jan S. Hesthaven [†]

abstract

In this paper we examine the merits of using Prolate Spheroidal Wave functions as basis functions in pseudospectral solution of hyperbolic partial differential equations.

The relevant approximation theory is being reviewed and some new results of approximations in Sobolev spaces are established. An optimal choice of the number of points required for a given bandwidth is derived.

Our conclusion is that one might gain from using the PSW functions over the traditional Chebyshev or Legendre methods in terms of accuracy and efficiency for marginally resolved broad band solutions.

[1]The work of the second author (DG) was partly supported by NSF under contract DMS-0207451 and by HyperComp under contract HPC/F33615-01-c-1866. The work of the last author (JSH) was partly supported by NSF under contract DMS-0074257 and through an NSF Career Award, by ARO under contract DAAD19-01-1-0631 and by the Alfred P. Sloan Foundation through a Sloan Research Fellowship.

[2]Division of Applied Mathematics, Brown University, Box F, Providence, RI 02912 (cqy@cfm.brown.edu, dig@cfm.brown.edu, jansh@cfm.brown.edu).

Pseudospectral methods([2][8]) involve approximating the solution of a PDE by polynomials (Chebyshev or Legendre, mostly) or trigonometric polynomials. The reason for their success is the spectral accuracy, i.e., the convergence rate depends only on the smoothness of the functions being approximated. This comes with a price: the norm of the differentiation matrix is proportional to the square of the number of interpolation points (or the order of the polynomial), resulting in small time steps ($\sim N^{-2}$) ([9]), when using explicit schemes.

In this paper we assess the performance of a pseudospectral method based on the Prolate Spheroidal Wave functions (PSWF - ψ_k^c) rather than on polynomials. In [15], the authors demonstrate the merits of using PSWFs for the interpolation, integration(quadrature), and differentiation of band limited functions. They show, among other things, that for a prescribed accuracy, less grid points are needed for interpolation and integration as compared to Chebyshev polynomials. Furthermore, the differentiation matrix has a smaller condition number. In this paper, we attempt to explore these properties in the context of solving hyperbolic partial differential equations. The first step in this direction is to review and expand the relevant approximation theory. We study the number of points per wave length required for a meaningful calculation and show that the coefficients in the expansion

$$e^{im\pi x} = \sum_{j=0}^{\infty} \hat{u}_j \psi_j^c(x)$$

decay exponentially fast if $c = m\pi$ and $j > \frac{2c}{\pi}$, i.e., only two points per wave length are needed. We then derive a new formula that demonstrates the spectral accuracy of approximations of smooth functions by PSWF. Several variants of pseudospectral PSWF methods based on different interpolation points are given. The first is based on the Gauss Lobatto points while the second method uses the zeroes of $(1-x^2)(\psi_N^c)'$ as grid points. The performance of those methods are essentially equivalent. We then apply the methods to a scalar hyperbolic equations and as well as hyperbolic systems.

The results of our study can be summarized as follows:

- The optimal choice of the number of grid points is $N = c$ where c is the bandwidth.

- With this choice one observes spectral accuracy. When the solution is broadband and marginally resolved, the PSWF based method is more accurate than the Chebyshev method with the same number of terms.

- Theoretically the time step Δt can be taken as $O(N^{-\frac{3}{2}})$. However the accuracy deteriorates. A robust choice implies $O(N^{-2})$.

The paper is organized as follows: In Section 1, we present some mathematical background for Prolate Spheroidal Wave Functions. Section 2 contains the new approximation results. In Section 3, we construct pseudospectral methods based on PSWF, we discuss their stability and solve scalar hyperbolic equations as well as hyperbolic systems. In the appendix, we give the proof for the new approximation results.

1 Preliminaries

In this section, we summarize the notation and some general results regarding the Prolate Spheroidal Wave Functions etc.

1.1 Prolate Spheroidal Wave Functions

Function $f : [-1, 1] \to [-1, 1]$ is band-limited if there exists a $c > 0$ and a function $\phi \in L^2[-1, 1]$ such that

$$f(x) = F_c(\phi)(x) = \int_{-1}^{1} e^{icxt}\, \phi(t)\, dt \tag{1.1}$$

It is easy to see that F_c: $L^2[-1, 1] \to L^2[-1, 1]$ is a compact operator, i.e., it has eigenvalues $\lambda_0, \lambda_1, \lambda_2, \cdots$, ordered as $|\lambda_{i-1}| \geq |\lambda_i|$, $\forall i > 0$. Denote by $\psi_j^c(x)$ the eigenfunction corresponding to λ_j. Then

$$\lambda_j\, \psi_j^c(x) = \int_{-1}^{1} e^{icxt}\, \psi_j^c(t)\, dt, \qquad x \in [-1, 1] \tag{1.2}$$

These eigenfunctions $\{\psi_j^c\}_{j=0}^{+\infty}$ are the Prolate Spheroidal Wave Functions(PSWF). We normalize them so that $\|\psi_j^c(x)\|_{L_2[-1,1]} = 1$. One can check that PSWFs satisfy the following equation

$$\mu_j\, \psi_j^c(x) = \int_{-1}^{1} \frac{\sin(c \cdot (x - t))}{x - t}\, \psi_j^c(t)\, dt, \qquad x \in [-1, 1]$$

where

$$\mu_j = \frac{c}{2\pi} \cdot |\lambda_j|^2 \tag{1.3}$$

Given any $c > 0$, the following theorem gives some properties of Prolate Spheroidal Wave functions(see [13], [15], and references therein):

Theorem 1 *$\psi_0^c(x)$, $\psi_1^c(x)$,$\cdots$ are real, orthonormal, smooth, and complete in $L^2[-1, 1]$, and form a Chebyshev system([11]) on $[-1, 1]$. Even-numbered ones are even functions; odd-numbered ones are odd functions. $\lambda_j = i^j|\lambda_j| \neq 0$, i is the complex unit. Among $\{\mu_j\}_{j=0}^{\infty}$, about $2c/\pi$ are very close to 1; order log(c) decay exponentially from 1 to nearly 0; the remaining are very close to zero.*

More importantly, there exists a strictly increasing positive sequence $\chi_0, \chi_1, \cdots$, s.t.

$$\left((1-x^2)(\psi_j^c(x))'\right)' + (\chi_j - c^2x^2)\psi_j^c(x) = 0 \tag{1.4}$$

When $c = 0$, the above equation reduces to the singular Sturm-Liouville problem with $p(x) = 1 - x^2$, $q(x) = 0$ and $\omega(x) = 1$, i.e., the PSWFs with $c = 0$ become the normalized Legendre polynomials([8], [2]). Following [15], we can evaluate $\psi_j^c(x)$ by expanding it as

$$\psi_j^c(x) = \sum_{k=0}^{\infty} \beta_k^j \cdot \overline{P_k(x)} \qquad j = 0, 1, 2, \cdots \tag{1.5}$$

where $\overline{P_k(x)}$ is the normalized Legendre polynomial of degree k. We substitute (1.5) into (1.4) and use the properties of Legendre polynomials to obtain an eigen problem:

$$(A - \chi_j \cdot I)\beta^j = 0 \tag{1.6}$$

Here A has the form([15]):

$$\begin{cases} A_{k,k} &= k(k+1) + \frac{2k(k+1)-1}{(2k+3)(2k-1)} \cdot c^2 \\ A_{k,k+2} &= \frac{(k+2)(k+1)}{(2k+3)\sqrt{(2k+1)(2k+5)}} \cdot c^2 \\ A_{k+2,k} &= A_{k,k+2} \end{cases} \tag{1.7}$$

for $k = 0, 1, 2, \cdots$, where the remainder of the entries of A are zero.

Since $\psi_j^c(x)$ is smooth, the coefficients β_k^j decay superalgebraically w.r.t. k. The following theorem([15]) tells us where to cut off in (1.5) for a certain accuracy when approximating $\psi_j^c(x)$.

Theorem 2 *Assume $\psi_m^c(x)$ is the m^{th} PSWF with band limit c, and λ_m is the eigenvalue corresponding to $\psi_m^c(x)$. If*

$$k \geq 2(\lfloor e \cdot c \rfloor + 1) \tag{1.8}$$

Then for all integer $m \geq 0$ and $c > 0$,

$$\left| \int_{-1}^{1} \psi_m^c(x) \overline{P_k(x)} dx \right| < \frac{1}{\lambda_m} \left(\frac{1}{2}\right)^{k-1}$$

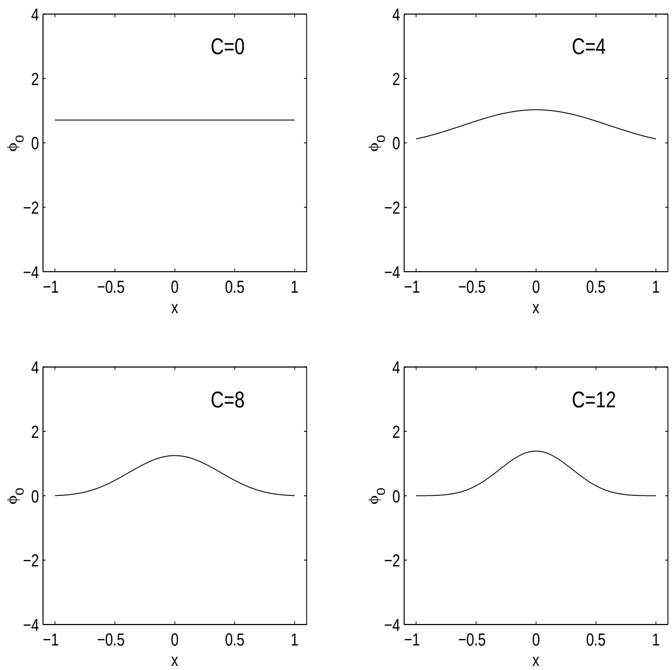

Figure 1: $\psi_0(x)$ under different c

Moreover, given any $\epsilon > 0$*, if*

$$k \geq 2(\lfloor e \cdot c \rfloor + 1) + \log_2\left(\frac{1}{\epsilon}\right) + \log_2\left(\frac{1}{\lambda_m}\right) \tag{1.9}$$

then

$$\left| \int_{-1}^{1} \psi_m^c(x)\overline{P_k(x)}dx \right| < \epsilon$$

□

With this algorithm, we compute two PSWF's (Figure 1 and 2) under different parameter c. From these two pictures, we can see that the roots of the PSWF move to the middle as c increases. This property suggests that by choosing $c > 0$ the PSWF needs less points per wavelength to accurately resolve a wave problem than Chebyshev/Legendre method. However, it also suggests that if c becomes too large for a fixed N, the PSWF is unable to represent functions defined on the whole interval.

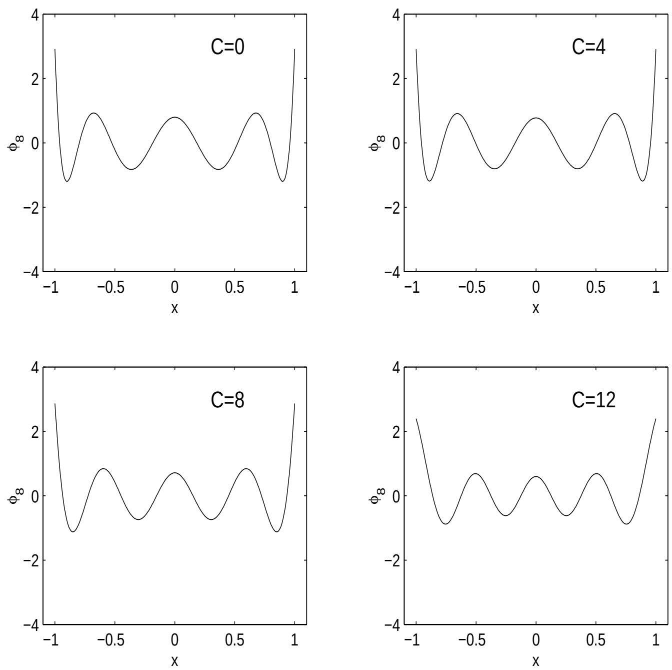

Figure 2: $\psi_8(x)$ under different c

2 Approximation

In this section, we explore the approximation properties of Prolate Spheroidal Wave Functions. We first show that for the single wave $\cos(m\pi x)$, with the optimal $c = m\pi$, the continuous PSWF expansion converges exponentially fast when at least 2 PSWF's are retained per wavelength. Equivalently 2 points per wavelength are required for exponential convergence of the discrete approximation. This should be compared with about π points per wavelength for Chebyshev/Legendre polynomials. The second result pertains to the approximation of smooth functions with a finite series of PSWF. In this case the optimal bandwidth parameter c is related to the number of points N. Our experiments show that the choice $c = N$ is a good choice if we want to maintain the full accuracy (16 digits) and we explain why we can not use $c \geq (\pi/2)N$.

2.1 Approximation of waves - Points per Wavelength

Consider the wave $u(x) = e^{im\pi x}$. It follows directly from (1.2) that its PSWF expansion is given as

$$e^{im\pi x} = \sum_{j=0}^{+\infty} \left(\lambda_j \psi_j^c(1)\right) \cdot \psi_j^c(x), \tag{2.1}$$

where $c = m\pi$.

To establish the exponential decay of the expansion coefficients for $j > \frac{2c}{\pi} = 2m$, note that

$$|\lambda_j \psi_j^c(1)|^2 = |\lambda_j||\lambda_j \psi_j^c(1)^2|$$

The term $\lambda_j \psi_j^c(1)^2$ is the j^{th} term in the expansion of $e^{i\pi m}$ (consult (2.1)) and therefore it is bounded (in fact it tends to zero with growing j). From [12], we know that $|\lambda_j^c|$ decays exponentially in j if $j > \frac{2c}{\pi}$ establishing the result: *The accurate resolution of a wave requires 2 PSWF's per wave.* We recall here that expansions with Chebyshev or Legendre polynomials require about π points per wave.

In Figure 3 we present the L_2 error in the PSWF expansion of the function $\cos(M\pi x)$,

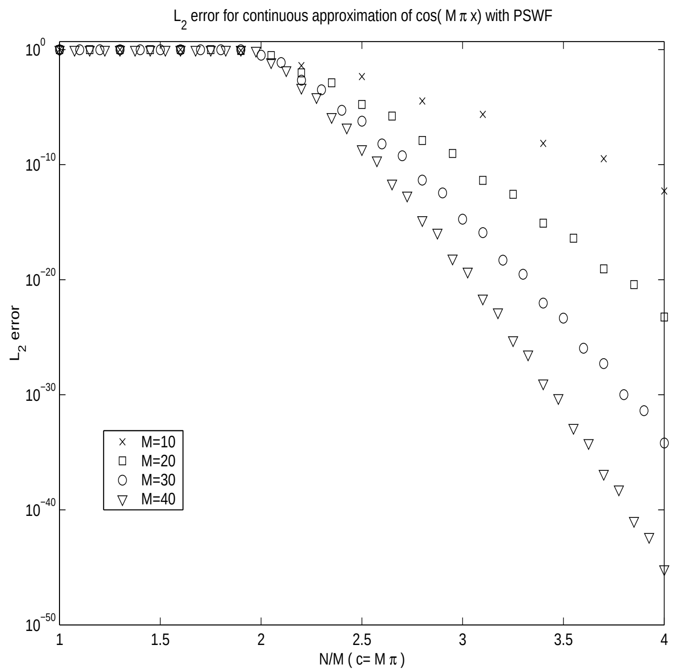

Figure 3: A plot of the L_2-error in the PSWF expansion of $\cos(M\pi x)$ truncated after N PSWF's versus N/M. $\times$: $M = 10$; $\square$: $M = 20$; $\bigcirc$: $M = 30$; $\bigtriangledown$: $M = 40$.

as a function of $\frac{N}{M}$ where N is the number of terms in the expansion. It clearly conforms that when $N/M > 2$ the error decays exponentially.

In the above discussion one takes $c = m\pi$ which is optimal. However for general functions, we do not have a simple optimal c. For example, in Figure 4, we give the interpolation results with PSWF for two different functions. Clearly, the best c depends on the specific function to be approximated and on the required accuracy. This is because any general function has many different modes, and each mode has an optimal c.

2.2 Error Estimates

In this Section, we consider error estimates, in the Sobolev norm, of the PSWF expansion of a smooth function. Let $x \in [-1, 1]$, consider the expansion $u(x) = \sum_{k=0}^{+\infty} \hat{u}_k \psi_k^c(x)$. The order of the convergence of the partial sum $\sum_{k=0}^{N} \hat{u}_k \psi_k^c(x)$ is determined by the decay rate of the coefficients $\hat{u}_k$.

In the appendix we prove

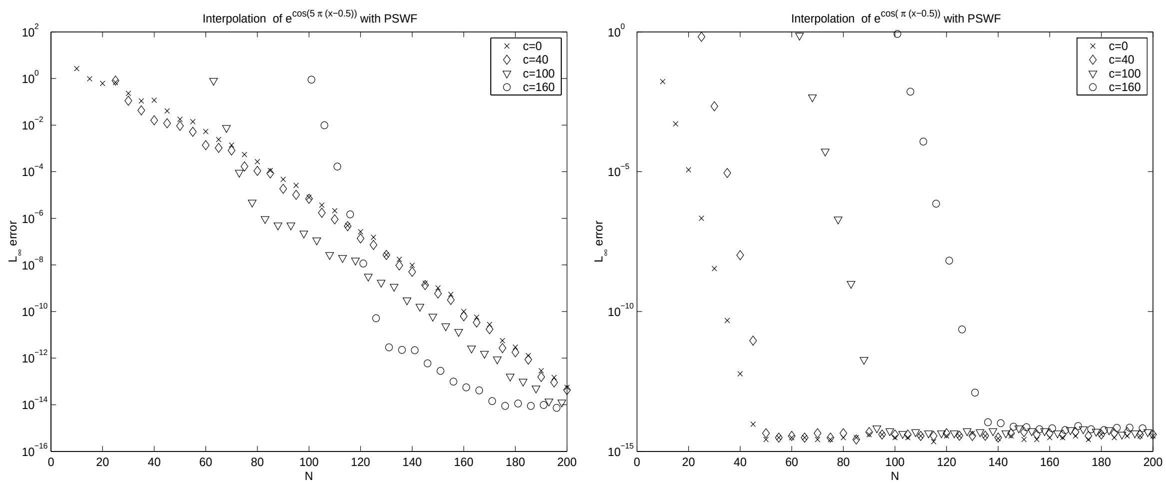

Figure 4: A plot to demonstrate that the optimal c, if it exists, depends on the specific problem and the required accuracy. Left: L_∞ error for the interpolation of $e^{\cos(5\pi(x-0.5))}$. For an error around 10^{-6}, $c = 100$ is the best one in the picture. For an error as small as 10^{-10}, $c = 160$ is optimal. Right: L_∞ error for the interpolation of $e^{\cos(\pi(x-0.5))}$, $c = 0$(Legendre base) is the best among the four choices.

Theorem 3 *Let $u(x) \in H^s[-1,1]$ with the PSWF expansion: $\sum_{i=0}^{+\infty} \psi_i^c(x)\hat{u}_k$, Denote by $\Lambda = \chi_N$(defined in Section 1), $q_N = \sqrt{\frac{c^2}{\chi_N}} < 1$, then*

$$|\hat{u}_N| \le D\left(N^{-\frac{2}{3}s}\|u\|_{H^s[-1,1]} + q_N^{\delta N}\ \|u\|_{L^2[-1,1]}\right) \tag{2.2}$$

where $\delta > 0$ and D are constants. □

From (2.2) it is evident that the expansion coefficient $\hat{u}_N$ decay faster than algebraically if $q_N < 1$. In this case terminating the sum at $n = N$ yields spectral accuracy. In [14], it is shown that if n grows with c as:

$$n = \frac{2}{\pi}\left[c + b\,\log\,(2\sqrt{c})\right], \tag{2.3}$$

then

$$\chi_n \sim c^2 + 2bc + O(1). \tag{2.4}$$

Thus

$$q_n < 1 \Leftrightarrow \chi_n > c^2 \Leftrightarrow \delta > 0 \Leftrightarrow b > 0 \Leftrightarrow n > \frac{2}{\pi}c. \tag{2.5}$$

To summarize:

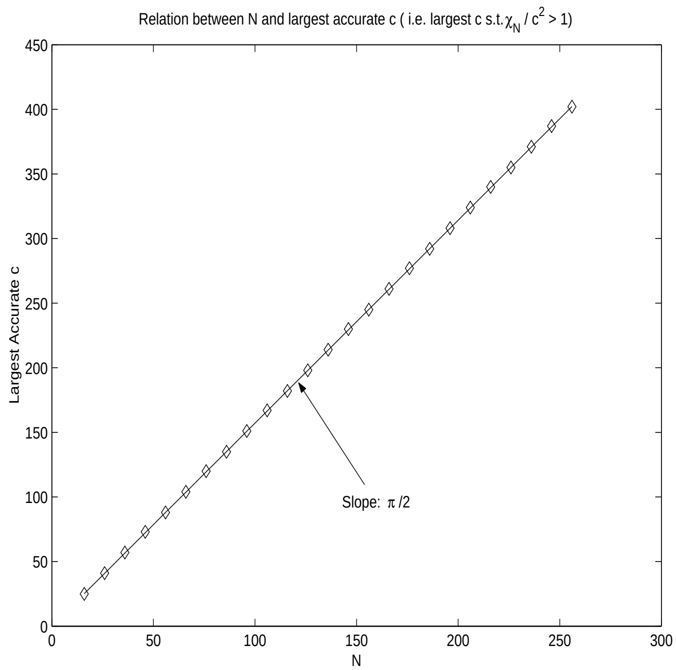

Figure 5: Relation between N and the biggest c which makes $q_N \leq 1$. The slope is $\pi/2$.

Theorem 4 *The error in the finite PSWF expansion of a smooth function* $u(x)$

$$\|u(x) - \sum_{n=0}^{N} \hat{u}_n \psi_n^c(x)\|_{L^2[-1,1]}$$

is spectrally small if

$$N > \frac{2}{\pi} c.$$

□

In Figure 5 we display the relationship between N and c such that $q_N < 1$, while Fig 6 shows the loss of accuracy as N approaches $\frac{2}{\pi}c$. We note here that the choice $c = N$ (which guarantees that q_N is bounded away from 1) seems a good choice if we require maximum accuracy. In Section 3, we will further discuss how to choose c, from the aspect of stable time-steps.

Similar results are obtained if one uses the PSWF to interpolate a smooth function. In Figure 7 we compare interpolations based on PSWF and Chebyshev polynomials. Here we chose the number of grid points $N = c$.

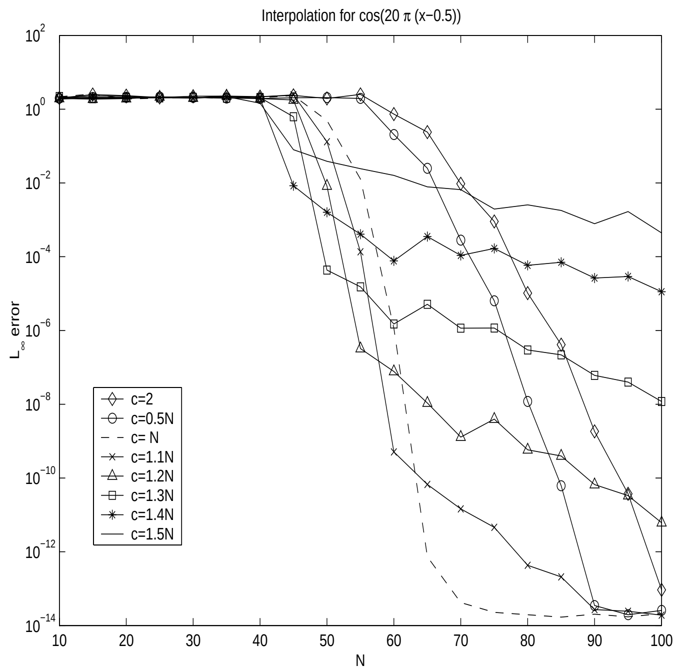

Figure 6: The loss of accuracy as c approaches $\frac{\pi}{2}N$.

For single mode function, e.g. $\cos(m\pi x)$, when $c = m\pi$, two points per wavelength are required for fast convergence.

The results indicate that the PSWF interpolation are superior for functions with fine structures.

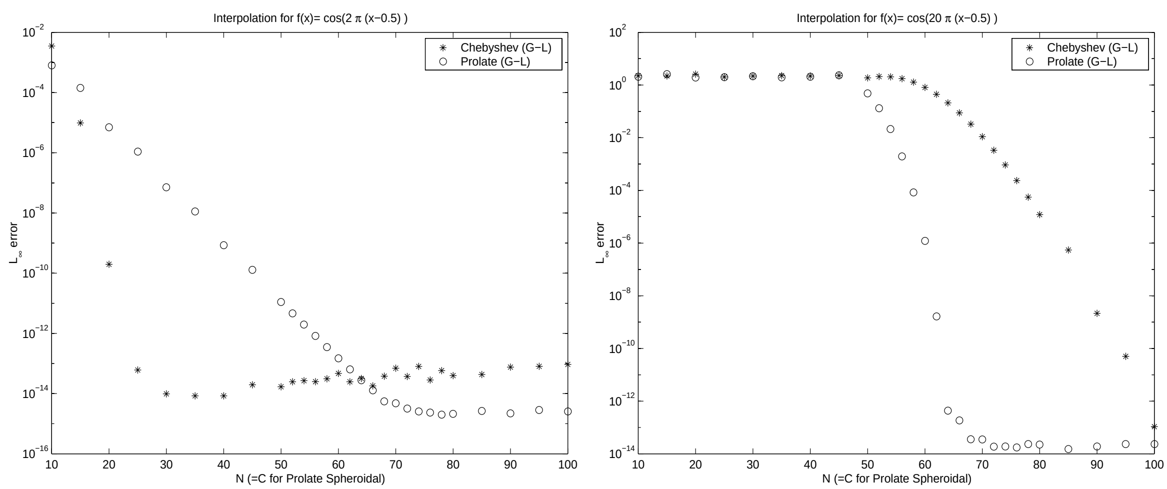

Figure 7: Interpolation results. 'o': Prolate Spheroidal Wave basis; '*' : Chebyshev polynomials basis. $c = N$ for Prolate Spheroidal Wave basis. Left: $f(x) = \cos(2\pi(x - 0.5))$; Right: $f(x) = \cos(20\pi(x - 0.5))$

3 Solving Partial Differential Equations

3.1 First Order Wave Equation

Consider the first order wave equation:

$$\begin{cases} u_t &= u_x \qquad x \in [-1,1] \\ u(1,t) &= g(t) \\ u(x,0) &= f(x) \end{cases} \tag{3.1}$$

Our approach is motivated by ([15]). Consider the points $x_0, ..., x_N$ to be specified later. We define the Prolate-Lagrange function as $L_j(x) = \sum_0^N l_{jk}\psi_k^c(x)$ such that $L_j(x_k) = \delta_{jk}$. The existence of Prolate-Lagrange functions follows from the fact that the PSWF form a Chebyshev system.

In the Galerkin approximation we seek an approximation of the form

$$u_N(x,t) = \sum_{j=0}^{N} u_N(x_j,t)L_j(x)$$

such that the vector $\vec{U} = (u_N(x_0), ..., u_N(x_N)))^T$ satisfies the equation

$$M\frac{d\vec{U}}{dt} = S\vec{U} - \tau(u_N(1,t) - g(t))\vec{e}_N. \tag{3.2}$$

Here, the boundary condition is imposed in a penalty way ([3], [7], [10]). The matrices $M = m_{jk}$ and $S = s_{jk}$ are defined as

$$m_{jk} = \int_{-1}^{1} L_j(x)L_k(x)dx \tag{3.3}$$

$$s_{jk} = \int_{-1}^{1} L_j(x)L_k^{'}(x)dx \tag{3.4}$$

and $\vec{e}_N = (0, ..., 1)$.

Theorem 5 *(Stability) The semi-discretized method described in (3.2) is stable for* $\tau \geq 1/2$.

Proof: For the stability proof we assume that $g(t) = 0$. Multiplying (3.2) by U^T we get

$$\begin{aligned}
\vec{U}^T M \vec{U} &= \sum_{jk} u_N(x_j) s_{kj} u_N(x_k) - \tau u_N(1,t)^2 \\
&= \sum_{jk} \int_{-1}^{1} u_N(x_j) u_N(x_k) L_j(x) L_k'(x) dx - \tau u_N(1,t)^2 \\
&= \int_{-1}^{1} u_N(x,t) \frac{\partial u_N(x,t)}{\partial x} - \tau u_N(1,t)^2 \\
&= \frac{1}{2} \left(u_N(1,t)^2 - u_N(-1,t)^2 - 2\tau u_N(1,t)^2 \right)
\end{aligned}$$

Thus, if $\tau \geq \frac{1}{2}$ then

$$\frac{d}{dt} \sum_{jk} \int_{-1}^{1} u_N(x_j) u_N(x_k) L_j(x) L_k(x) dx \leq 0$$

or

$$\frac{d}{dt} \int_{-1}^{1} u_N(x,t)^2 dx \leq 0.$$

Proving the theorem. ■

Comment: In the collocation method we replace the integrals by quadrature formulas based on the points x_k. The points used are either the Gauss Lobatto PSWF points(one way to compute these points is given in [4]) or the zeroes of $(1 - x^2)(\psi_N^c)'$. The performance of these two methods is about the same. For the latter case, however, we do not have a stability proof. We verified numerically that the eigenvalues of the differentiation matrix have negative real parts.

When using explicit time discretization (the most popular being the Runge-Kutta schemes) one faces a stability limit on the time step Δt. A necessary condition for stability is the product of Δt and the largest eigenvalue of the matrix $M^{-1}(S - \tau \vec{e}_N \vec{e}_N^T)$ is in the stability region of the RK scheme.

From Figure 8, one can see that the largest eigenvalue λ of PSWF collocation decreases when c/N increases. Thus it appears that we should use the largest possible c to maximize Δt. This is is confirmed by figure 9. The biggest stable time-step approaches a growth rate like $O(N^{-\frac{3}{2}})$, when c goes to $(\pi/2)N$. It seems that one can use a time-step of order $O(N^{-\frac{3}{2}})$

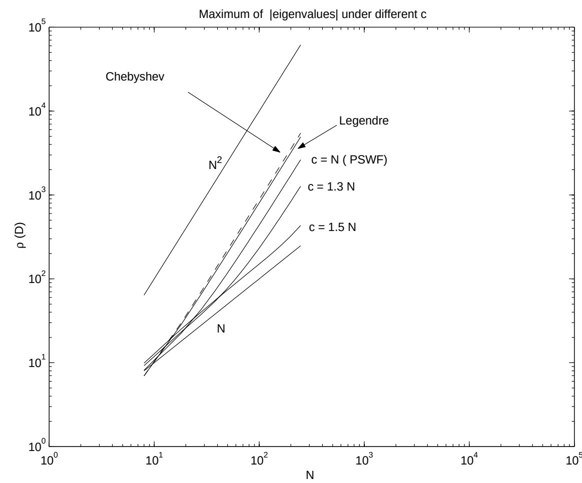

Figure 8: Largest absolute value of PSWF collocation under different $c's$, and compared with Chebyshev and Legendre collocation.

by letting $c = (\pi/2)N$. However, as established in Section 2, this choice of c causes a loss of accuracy as demonstrated in Figure 6. In Table 1, we give the errors for the time-steps in Figure 9. It is evident that the accuracy is decreasing when c approaches $(\pi/2)N$. This is consistent with our analysis for the approximation with PSWF.

Table 1: L_∞ error when solving $u_t = u_x$ for $u(x,t) = \cos(2\pi(x + t - 0.5))$ with collocation methods. 10-th order explicit Runge-Kutta is used. For each N of each method, Δt is just the biggest stable time step from figure 9

N	80	120	160	200
Chebyshev	3.453×10^{-14}	4.952×10^{-14}	1.521×10^{-13}	1.115×10^{-13}
Legendre	7.361×10^{-14}	1.117×10^{-12}	1.274×10^{-12}	1.592×10^{-12}
PSWF(c=N)	9.770×10^{-15}	9.104×10^{-15}	2.081×10^{-14}	1.482×10^{-14}
PSWF(c=1.3N)	3.638×10^{-1}	2.860×10^{-9}	7.133×10^{-12}	9.137×10^{-14}
PSWF(c=1.5N)	5.022×10^{-2}	2.968×10^{-1}	8.051×10^{-2}	1.649×10^{-4}

As a compromise, we use $c = N$ in all subsequent numerical tests. This yields a time-step which is twice the one obtained by the Legendre collocation method. Furthermore, for any case, one may use different values for the constant c to get more benefits, e.g., in Figure 6, $c = 1.1N$ could be used if only about 10^{-9} accuracy is required.

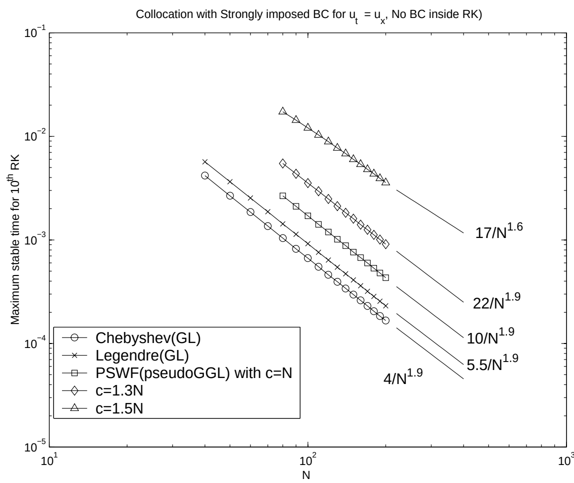

Figure 9: Biggest stable time-steps for PSWF Collocation under different $c's$, and compared with Chebyshev and Legendre Collocation. 10^{th} explicit Runge-Kutta scheme is used.

3.1.1 Numerical Tests

All the following numerical tests are carried out by a collocation method in which we seek an approximation $u_N = \sum_{j=0}^{N} \tilde{u}_j \psi_j^c(x)$ such that the equation

$$\frac{\partial u_N}{\partial t} - \frac{\partial u_N}{\partial x} = 0$$

at the grid points x_j. The boundary condition is applied either strongly or by a penalty procedure.

We considered three different initial conditions $f(x)$: The Heaviside function $H(x)$ is

Table 2:

smooth	non-smooth
$\cos(2\pi(x-0.5))$	
$\cos(20\pi(x-0.5))$	$\sin(20\pi(x-0.5)) + H(x-0.5)$

defined as:

$$H(x) = \begin{cases} 1 & \text{if} \quad x \leq 0 \\ -1 & \text{otherwise} \end{cases} \tag{3.5}$$

In Figure 10 we show the error in the solution of (3.1) with the smooth initial condition. The results show that as in the case of interpolation, the Chebyshev method performs better

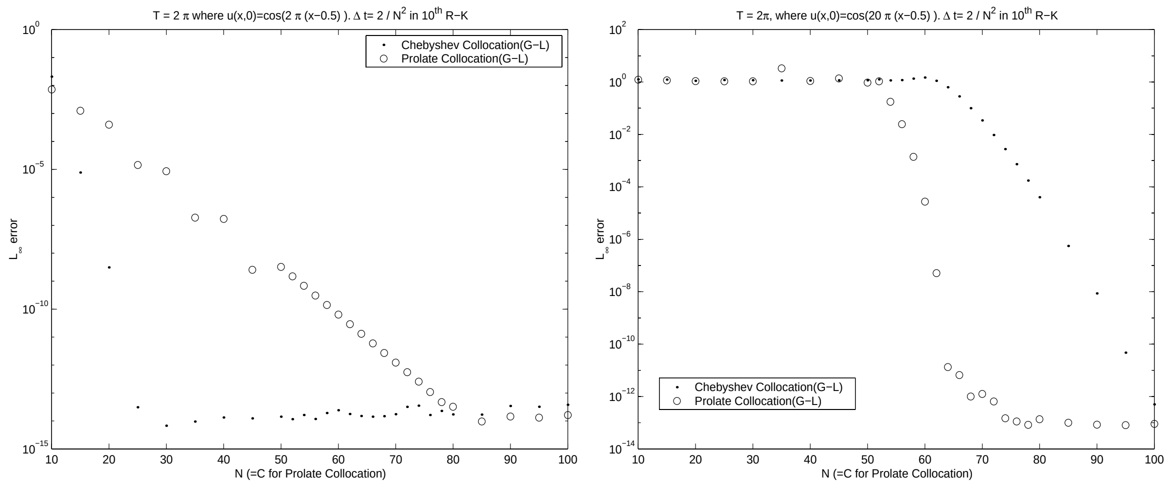

Figure 10: Solving $u_t = u_x$ with smooth initial conditions by Collocation method with strongly imposed boundary condition. Left: $u(x,t) = \cos(2\pi(x - 0.5 + t))$; Right: $u(x,t) = \cos(20\pi(x-0.5+t))$ Final time: $T = 2\pi$. 10^{th} order Runge-Kutta with $\Delta t = \frac{2}{N^2}$. 'o': Prolate Spheroidal Wave basis; '.' : Chebyshev polynomials basis. $c = N$ for Prolate Spheroidal Wave basis.

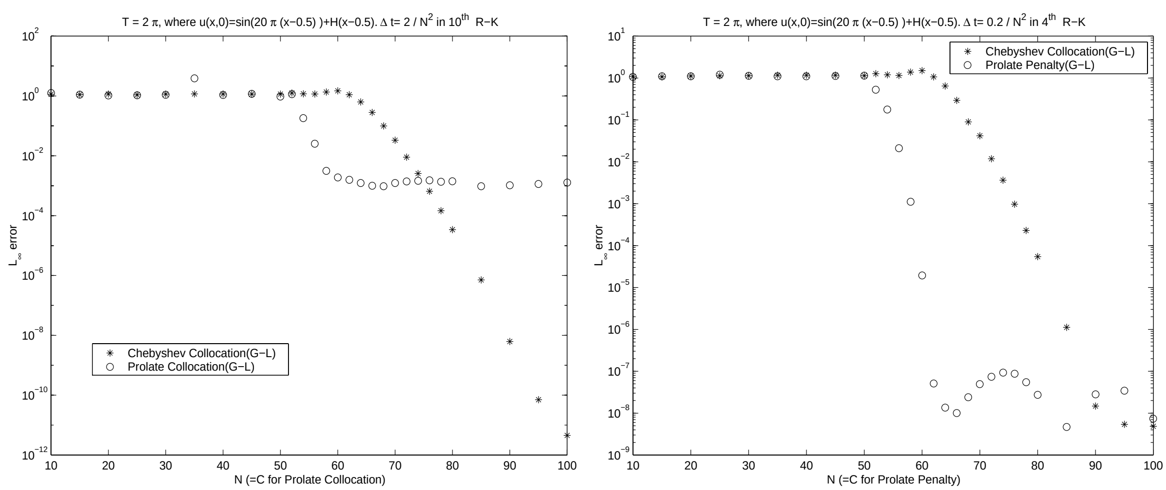

Figure 11: Solving $u_t = u_x$ with discontinuous initial condition by Collocation method. Left: Strongly imposed boundary condition for both Chebyshev and Prolate Spheroidal collocation, 10^{th} order Runge-Kutta with $\Delta t = \frac{2}{N^2}$; Right: Weakly imposed boundary condition for Prolate Spheroidal collocation, 4^{th} order Runge-Kutta with $\Delta t = \frac{0.2}{N^2}$; Final time: $T = 2\pi$ and $u(x,0) = \sin(20\pi(x - 0.5)) + H(x - 0.5)$. 'o': Prolate Spheroidal Wave basis; '*' : Chebyshev polynomials basis. $c = N$ for PSWF collocation.

for a small number of waves, whereas the PSWF method is clearly better for a large number of waves.

In Figure 11 we present the error for the discontinuous, initial condition. In this case the solution itself is discontinuous and the point of discontinuity propagates towards the boundary with the fixed speed $a = 1$.

We observe that the error does not decay below 10^{-4}. The reason for that is that the boundary condition was imposed strongly, i.e., the numerical solution satisfied the boundary condition at any time step. When the boundary condition is imposed in the weak form as in ([3], [10], [7]) the PSWF method is superior to the Chebyshev method. This is demonstrated in the right part of Figure 11.

A possible reason for the better performance of the weak imposition of the boundary condition might be linked to the behavior of the differentiation matrix. Figures 12 and 13 show the spectrum of the modified differentiation matrix for PSWF collocation with strongly and weakly imposed boundary conditions respectively. The positive real parts in Figure 12 are caused by the round-off errors. From these results, we can see the importance of imposing boundary conditions in a penalty way. The same phenomenon is observed when using the Legendre collocation method to solve the equation with discontinuous initial condition.

3.2 Cavity problem

In this section, we solve the one-dimensional Maxwell equation:

$$\begin{cases} \epsilon \frac{\partial E}{\partial t} & = \frac{\partial H}{\partial x} \\ \mu \frac{\partial H}{\partial t} & = \frac{\partial E}{\partial x} \end{cases} \tag{3.6}$$

where $E(x,t)$ and $H(x,t)$ are the electric and magnetic fields, and ϵ and μ are the relative permitivity and permeability of the materials. Specially, we consider the following test case: a one-dimensional cavity $[-1, 1]$ is filled with two di-electric media with a material interface at $x = 0$. The two perfectly conducting walls are located at $x = -1$ and $x = 1$. Denote by ϵ_1 and μ_1 the relative permitivity and permeability of the material at $[-1, 0]$. Similarly, ϵ_2

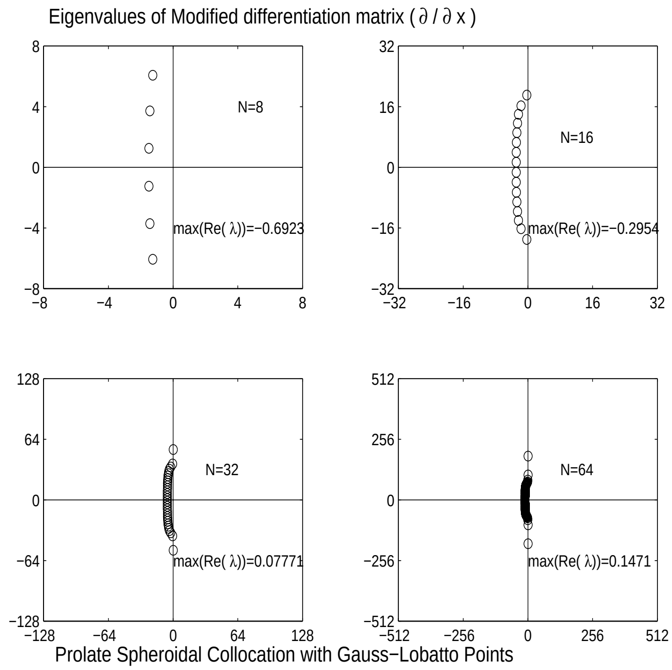

Figure 12: Eigenvalues of modified differential matrix for PSWF collocation, with strongly imposed boundary condition.

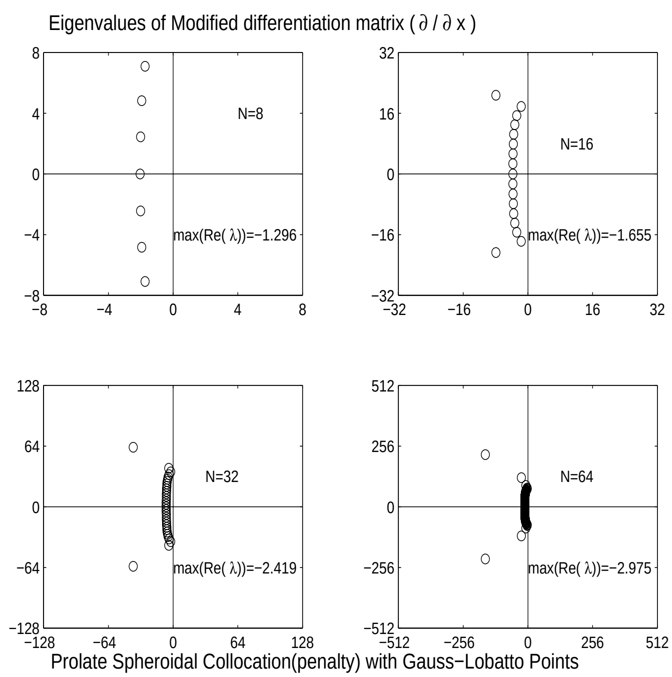

Figure 13: Eigenvalues of modified differential matrix for PSWF collocation with penalty(weakly) way to implement Boundary Condition.

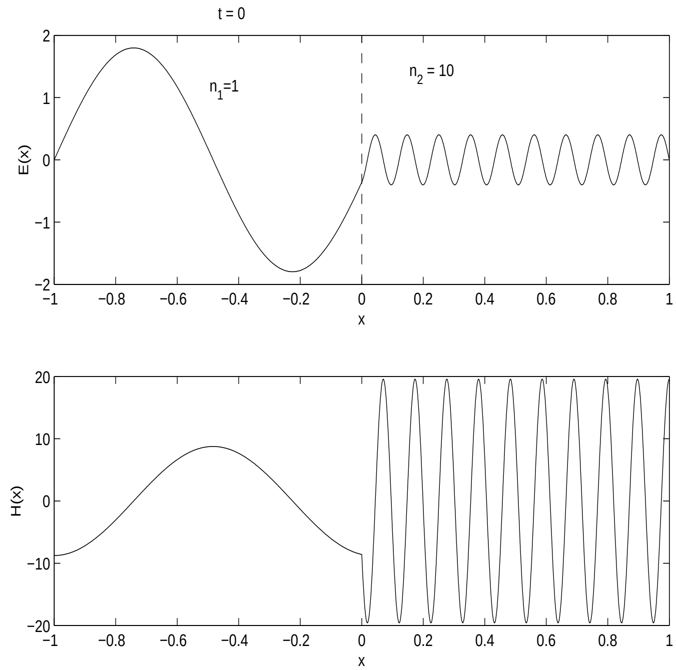

Figure 14: Exact solution at $t = 0$, $n_1 = 1.0$, $n_2 = 10.0$. Upper: electric field $E(x,t)$; Lower: magnetic field $H(x,t)$

and μ_2 are the relative permitivity and permeability of the material in $[0,1]$. The electric and magnetic fields in the two domain are denoted by E_1, H_1 and E_2, H_2.

Since the walls are perfectly conducting, the boundary conditions are:

$$E_1(-1,t) \quad = 0 \text{ or } \frac{\partial H_1}{\partial x}|_{x=-1} = 0 \tag{3.7}$$

$$E_2(1,t) \quad = 0 \text{ or } \frac{\partial H_2}{\partial x}|_{x=1} = 0 \tag{3.8}$$

If the interface has finite conductivity, the electric and magnetic fields, E and H, are continuous across the interface. Further, we assume $\mu_1 = \mu_2 = 1.0$ and denote $n_1 = \sqrt{\epsilon_1}$, $n_2 = \sqrt{\epsilon_2}$.

In Figure 14 we display the solution at $t = 0$. See [5] for the derivation of the exact solution. When $n_1 \neq n_2$, the solution loses smoothness at the material interface. It is only globally C^0 in the whole domain $[-1,1]$. Thus without using domain decomposition, we can only get at most second order convergence with Chebyshev or PSWF collocation method. Figure 15 is the results of Chebyshev and PSWF Collocation for $n_1 = 1, n_2 = 10$. Because of

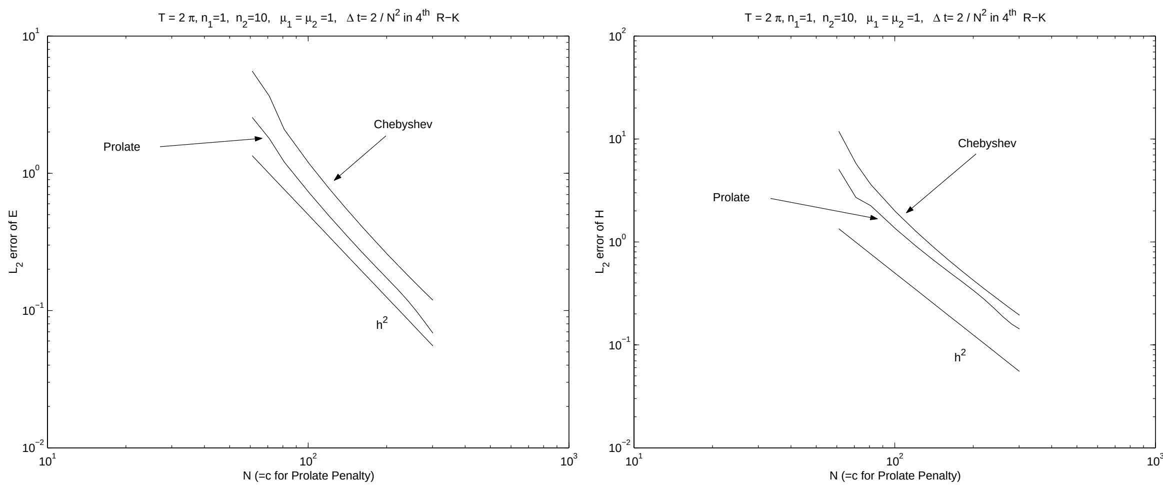

Figure 15: The discrete L^2-error at $t = 2\pi$. Strongly imposed boundary condition for Chebyshev collocation. Weakly imposed boundary condition for PSWF collocation. Left: electric field E(x,t); Right: magnetic field H(x,t).

the low order accuracy, there is not much gain in using PSWF collocation, although PSWF needs less points per wavelength to resolve the solution.

For both PSWF and Chebyshev collocations, there is a spike (Figure 16) propagating in the left half domain, whose speed is the speed of a characteristic wave. It is caused by the initial condition. To be more precise, the initial condition we use is from the exact solution for the partial differential equation. But the numerical scheme is an approximation of the original PDE. However, we can get the initial condition from the numerical scheme. Assume the semi-discretized equation of (3.6) is:

$$\begin{cases} \frac{d\vec{E}}{dt} & = D_H \, \vec{H} \\ \frac{d\vec{H}}{dt} & = D_E \, \vec{E} \end{cases} \tag{3.9}$$

Take the exact solution to the numerical scheme as :$\vec{E} = \tilde{\vec{E}} e^{i\omega t}$, $\vec{H} = \tilde{\vec{H}} e^{i\omega t}$, then plug into (3.9) to obtain:

$$i\omega \begin{pmatrix} \tilde{\vec{E}} \\ \tilde{\vec{H}} \end{pmatrix} = \begin{pmatrix} 0 & \tilde{\vec{H}} \\ \tilde{\vec{E}} & 0 \end{pmatrix} \tag{3.10}$$

This is an eigen problem. We can easily solve the above equation and use the solution as the initial condition of the scheme. As shown in Figure 17, this removes the spike.

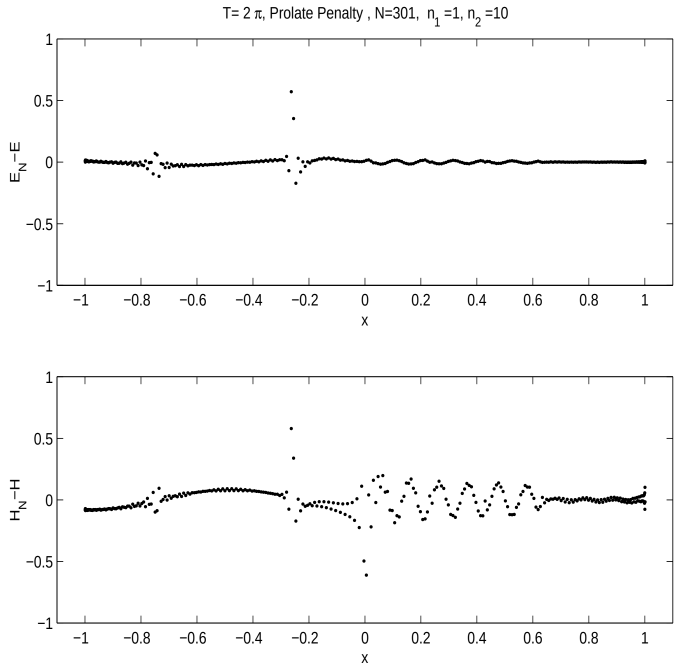

Figure 16: Error distribution for PSWF collocation. $(c =)N = 301$. $t = 2\pi$, $n_1 = 1.0$, $n_2 = 10.0$. Upper: electric field $E_N(x,t) - E(x,t)$; Lower: magnetic field $H_N(x,t) - H(x,t)$. Where $E_N(x,t), H_N(x,t)$ are the numerical solutions.

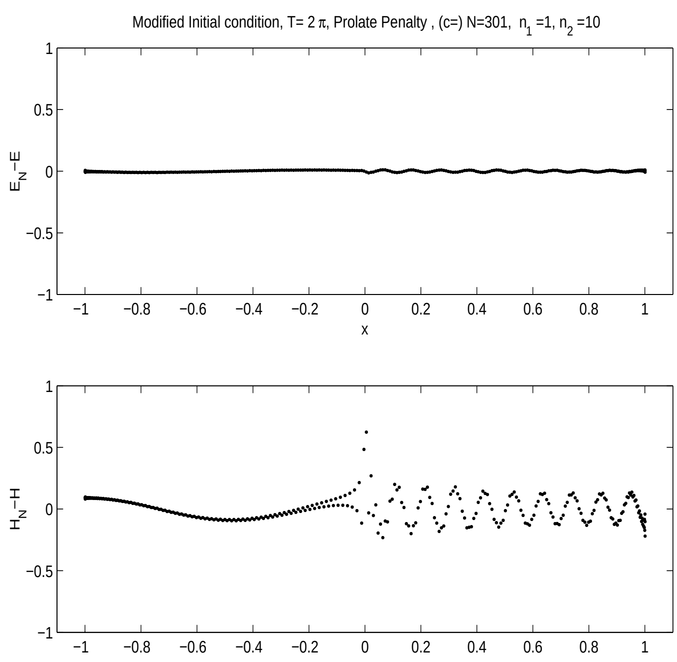

Figure 17: With modified initial condition. Error distribution for Prolate Spheroidal collocation. $(c =)N = 301$. $t = 2\pi$, $n_1 = 1.0$, $n_2 = 10.0$. Upper: electric field $E_N(x,t) - E(x,t)$; Lower: magnetic field $H_N(x,t) - H(x,t)$. Where $E_N(x,t), H_N(x,t)$ are the numerical solutions.

4 Conclusions

Our study of the applicability of PSWF based methods to the numerical solution of time dependent PDEs yields the main conclusions:

- The PSWF approximation requires two points per wavelength to resolve a single mode wave function ($\cos(m\pi x)$) if c is chosen as $c = m\pi$.

- Approximating a broad band function $u(x)$ by a finite expansion of the form $\sum_{n=0}^{N} \hat{u}_n \psi_n^c(x)$ one obtains spectral accuracy for $N > \frac{2}{\pi}c$, with loss of accuracy when N approaches the limit. A robust choice is $N = c$.

- When solving the wave equation $u_t = u_x$ with explicit temporal schemes, the CFL bound on the time-step increases if $c \leq (\pi/2)N$ increases. Asymptotically, $\Delta t = O(N^{-3/2})$ if c is very close to $(\pi/2)N$. However this choice results in a deterioration of the accuracy. We found that $c = N$ is good choice to ensure maximum accuracy and big stable time-step.

- For marginally resolved broad band problems, the PSWF based method with carefully chosen c is better than the Legendre/Chebyshev collocation methods: less points needed per wavelength for fast convergence and the allowable time-step is twice as the latter.

- The weak imposition of the boundary condition is necessary for the success of the method for problems with discontinuous initial conditions. By weakly applying the boundary condition, we improve the spectrum of the first order differentiation matrix of PSWF, i.e., moving those eigenvalues with almost zero real parts a little distance away from the imaginary axis.

In [1], Boyd got the similar results.

Acknowledgment The authors thank Boyd for showing his work [1] before publishing it.

Appendix

In the appendix, we prove Theorem 3.

Let $\beta_k = \beta_k^N$ be the coefficient in the expansion of $\psi_N^c(x)$ in terms of the normalized Legendre polynomials: $\psi_N^c(x) = \sum_{k=0}^{+\infty} \beta_k^N \overline{P_k(x)}$.

$$\beta_k = \int_{-1}^{1} \overline{P_k(x)} \psi_N(x) dx$$

The following recurrence relation for β_k was proven in [15].

$$\begin{aligned} \frac{(k+2)(k+1)}{(2k+3)\sqrt{(2k+5)(2k+1)}}\,\beta_{k+2} &= \left(\frac{\Lambda - k(k+1)}{c^2} - \frac{2k(k+1)-1}{(2k+3)(2k-1)}\right)\,\beta_k \\ &\quad - \frac{k(k-1)}{(2k-1)\sqrt{(2k-3)(2k+1)}}\,\beta_{k-2} \end{aligned} \tag{4.1}$$

We note that, from [14], $\Lambda = \chi_N = O(N^2)$. Let m be any integer satisfying

$$m = O(\Lambda^{1/3}) = O(N^{2/3}) \qquad \text{and} \qquad 2m(2m+1) < \frac{\ln 2}{2}\Lambda \tag{4.2}$$

Then we have

Lemma 1 *Let $q = q_N = \sqrt{\frac{c^2}{\Lambda}} < 1$, then for any given $k \le 2m$, the following bounds for β_k hold:*

$$|\beta_k| \le \begin{cases} D\left(\frac{2}{q}\right)^k |\beta_0| & \text{even } k \\ D\left(\frac{2}{q}\right)^k |\beta_1| & \text{odd } k \end{cases} \tag{4.3}$$

where D is a constant independent of m.

Proof: We only prove it for even k's. The proof for odd k is similar.

Rewrite (4.1) as

$$\beta_{k+2} = \frac{1}{f(k+2)}\left(\frac{1}{q^2}\left(1 - \frac{k(k+1)}{\Lambda}\right) - g(k)\right)\,\beta_k - \frac{f(k)}{f(k+2)}\,\beta_{k-2} \tag{4.4}$$

where $f(x) = \frac{x(x-1)}{(2x-1)\sqrt{(2x-3)(2x+1)}}$ and $g(x) = \frac{2x(x+1)-1}{(2x+3)(2x-1)}$.
It is easy to verify that

$$1/4 \le f(x) \le 2\sqrt{5}/15; \qquad \frac{1}{2} \le g(x) \le \frac{11}{21} \qquad \text{for } x \ge 2$$

Therefore $f(x)/f(x+2) \le 8\sqrt{5}/15$ when $x \ge 2$.

Since

$$k \le 2m \longrightarrow \frac{1}{q^2}\left(1 - \frac{k(k+1)}{\Lambda}\right) \ge \frac{1}{q^2}(1 - \frac{\ln 2}{2}) > \frac{11}{21} \ge g(x) \qquad \text{for } x \ge 2$$

The coefficient of β_k in (4.4) is positive and therefore if we assume (4.3) is true for $k, k-2$, we can bound β_{k+2} as

$$\begin{aligned}
|\beta_{k+2}| &\le \frac{1}{f(k+2)}\left(\frac{1}{q^2}\left(1 - \frac{k(k+1)}{\Lambda}\right) - g(k)\right) |\beta_k| + \frac{f(k)}{f(k+2)} |\beta_{k-2}| \\
&\le 4\frac{1}{q^2}\left(1 - \frac{\ln 2}{2}\right) D \left(\frac{2}{q}\right)^k |\beta_0| + \frac{8\sqrt{5}}{15} D \left(\frac{2}{q}\right)^{k-2} |\beta_0| \\
&\le D \left(\frac{2}{q}\right)^{k+2} \left(1 - \frac{\ln 2}{2} + \frac{\sqrt{5}q^4}{30}\right) |\beta_0| \le D \left(\frac{2}{q}\right)^{k+2} |\beta_0|
\end{aligned} \tag{4.5}$$

The last inequality follows from the fact that $q < 1$ and $1 - \frac{\ln 2}{2} + \frac{\sqrt{5}q^4}{30} < 1$. When $k = 0$ and 2, (4.3) can be easily satisfied by choosing the constant D. The lemma is proven. ■

Define

$$A_k = \int_{-1}^{1} x^k \psi_N^c(x)\, dx \tag{4.6}$$

One can check that $\sqrt{2}\beta_0 = A_0$ and $\sqrt{2/3}\beta_1 = A_1$.

Lemma 2 *Let m be an integer satisfying* (4.2)*, then,*

$$|A_0| \le K q^{2m} \sqrt{\frac{1}{2m}} \tag{4.7}$$

where K is a constant independent of m.

Proof: We first show that

$$|A_0| \le q^{2m} |A_{2m}| \prod_{l=1}^{m-1} \frac{1}{1 - \frac{2l(2l+1)}{\Lambda}} \tag{4.8}$$

We rewrite (1.4) as

$$\left((1-x^2)\psi'\right)' + \Lambda(1 - q^2x^2)\psi = 0$$

For $l \leq m$, multiply the above equation by x^{2l} , then integrate on [-1,1] to obtain

$$\begin{cases} 2l(2l-1)A_{2l-2} + (\Lambda - 2l(2l+1))\, A_{2l} - \Lambda q^2 A_{2l+2} & = 0 \qquad l \geq 1 \\ A_0 - q^2 A_2 & = 0 \qquad l = 0 \end{cases} \tag{4.9}$$

Since $2m(2m+1) \leq \Lambda$, all $A_0, A_2, \cdots, A_{2m+2}$ have the same sign. Thus

$$|A_{2l}| \leq q^2 \; |A_{2l+2}| \frac{\Lambda}{\Lambda - 2l(2l+1)} \leq q^2 \; |A_{2l+2}| \frac{1}{1 - \frac{2l(2l+1)}{\Lambda}}$$

Then (4.8) follows from induction.

To show (4.7), we note that $1 - x \geq e^{-2x}$ when $0 \leq x \leq \frac{\ln 2}{2}$. Therefore,

$$1 - \frac{2l(2l+1)}{\Lambda} \geq e^{-2\frac{2l(2l+1)}{\Lambda}} \qquad \text{for } l = 1, 2, \cdots, m-1$$

for m satisfying (4.2), leading to

$$\prod_{l=1}^{m-1} \frac{1}{1 - \frac{2l(2l+1)}{\Lambda}} \leq e^{\frac{\sum_{l=1}^{m-1} 4l(2l+1)}{\Lambda}} \leq e^{\frac{\frac{8}{3}m^3}{\Lambda}}$$

By (4.2), $m = O(\Lambda^{1/3})$. And (4.6) yields

$$|A_{2m}| \leq \|x^{2m}\|_{L^2[-1,1]} \; \|\psi\|_{L^2[-1,1]} \leq \sqrt{\frac{1}{2m}}$$

which proves (4.7). ■

In the same way, one can also show that $|A_1| \leq K q^{2m} \sqrt{\frac{1}{2m}}$ given the same conditions on m.

We are now ready to:

Proof of Theorem 3 : Assume $u(x)$ has the Legendre expansion:

$$u(x) = \sum_{k=0}^{+\infty} a_k P_k(x)$$

By definition,

$$\hat{u}_N = \int_{-1}^{1} u(x)\psi_N(x)dx = \int_{-1}^{1} \psi_N(x) \left(\sum_{k=0}^{+\infty} a_k P_k(x) \right) dx$$

Let M be an integer such that:

$$\frac{M+1}{2m} = \gamma \frac{\ln(1/q)}{\ln(2/q)} \tag{4.10}$$

where $0 < \gamma < 1$ is a constant. Denote by $u_M(x)$ the partial sum $u_M(x) = \sum_{k=0}^{M} a_k P_k(x)$, then

$$\hat{u}_N = \int_{-1}^{1} u_M(x)\ \psi_N(x) dx + \qquad \int_{-1}^{1} (u(x) - u_M(x))\ \psi_N(x) dx$$

We use I and II to represent the first and second term respectively. According to the error estimate of the Legendre approximation ([6][2]),

$$|II| \leq \|u - u_M\|_{L^2[-1,1]}\ \|\psi_N(x)\|_{L^2[-1,1]} \leq DM^{-S}\|u\|_{H^S[-1,1]}$$

where D is a constant (in the following, D is used for different constants). Now,

$$\begin{aligned}
|I| &= \left|\sum_{k=0}^{M} a_k \int_{-1}^{1} P_k(x)\psi_N(x)dx\right| = \left|\sum_{k=0}^{M} \left(a_k\sqrt{\frac{2}{2k+1}}\right)\ \left(\int_{-1}^{1} \overline{P_k(x)}\psi_N(x)dx\right)\right| \\
&\leq \left(\sum_{k=0}^{M}(a_k)^2\frac{2}{2k+1}\right)^{1/2}\ \left(\sum_{k=0}^{M}\left(\int_{-1}^{1}\overline{P_k(x)}\psi_N(x)dx\right)^2\right)^{1/2} \\
&\leq \|u\|_{L^2[-1,1]}\ \left(\sum_{k=0}^{M}\beta_k^2\right)^{1/2} \\
&\leq D\|u\|_{L^2[-1,1]}\ \left(\sum_{k=0}^{M}\left(\frac{2}{q}\right)^{2k}\right)^{1/2}\ \max\left(|\beta_0|, |\beta_1|\right)
\end{aligned}$$

From Lemma 2, $\beta_0 = \frac{1}{\sqrt{2}}A_0 < Kq^{2m}\sqrt{\frac{1}{2m}}$ and $\beta_1 = \sqrt{3/2}A_1 < Kq^{2m}\sqrt{\frac{1}{2m}}$, where K is a constant. So

$$\begin{aligned}
|I| &\leq D\|u\|_{L^2[-1,1]}\ \left(\sum_{k=0}^{M}\left(\frac{2}{q}\right)^{2k}\right)^{1/2}\ q^{2m}\sqrt{\frac{1}{2m}} && (4.11)\\
&\leq D\|u\|_{L^2[-1,1]}\ \left(\frac{2}{q}\right)^{M+1}\ q^{2m}\sqrt{\frac{1}{2m}} && (4.12)\\
&\leq D\|u\|_{L^2[-1,1]}\ \left(q\left(\frac{2}{q}\right)^{\frac{M+1}{2m}}\right)^{2m}\ \sqrt{\frac{1}{2m}} && (4.13)\\
&\leq D\|u\|_{L^2[-1,1]}\, p^{2m}\sqrt{\frac{1}{2m}} && (4.14)
\end{aligned}$$

where $p = q\left(\frac{2}{q}\right)^{\frac{M+1}{2m}}$.

From (4.10), $p = q^{1-\gamma}, \gamma < 1$ and $M = O(m) = O(N^{2/3})$. Combining the bounds for I and II, we get

$$|\hat{u}_N| \leq D\left(N^{-\frac{2}{3}S}\|u\|_{H^S[-1,1]} + q_N^{\frac{2}{3}(1-\gamma)N}\ \|u\|_{L^2[-1,1]}\right)$$

Proving Theorem 3 with $\delta = \frac{2}{3}(1 - \gamma)$. ■

References

[1] John P. Boyd *Prolate Spheroidal Wave functions as an Alternative to Chebyshev and Legendre Polynomials for Spectral Element and Pseudospectral Algorithms.* To be determined, (2003), To be submitted.

[2] C.Canuto, M.Y.Hussaini, A.Quarteroni and T.A. Zang, 1988, *Spectral Methods in Fluid Dynamics,* Springer-Verlag.

[3] M. H. Carpenter and D. Gottlieb, *Spectral Methods on Arbitrary Grids*, J. Comput. Phys. 129(1996), pp. 74-86.

[4] H. Cheng, V. Rokhlin, and N. Yarvin, *Nonlinear Optimization , Quadrature and Interpolation*, SIAM J. OPTIM. Vol. 9, No. 4, pp. 901-923 .

[5] A. Ditkowski, K, Dridi, and J.S. Hesthaven, *Convergent Cartesian Grid Methods for Maxwell's Equations in Complex Geometries*, Journal of Computational Physics 170, 39-80 (2001)

[6] D. Funaro , *Polynomial Approximation of Differential Equations.* Lecture Notes in Physics, m 8. Springer Verlag, Berlin. 1992.

[7] D. Funaro and D. Gottlieb, *A New Method of Imposing Boundary Conditions in Pseudospectral Approximations of Hyperbolic Equations*, Math. Comp. **51**(1988), pp. 599-613

[8] D. Gottlieb, M.Y. Hussaini and S.A. Orszag, 1984, Theory and application of spectral methods, in: R. Voigt, D. Gottlieb and M.Y. Hussaini, ds., *Spectral Methods for Partial Differential Equations*(SIAM-CBMS, Philadelphia, PA, 1984) pp. 1-94.

[9] D. Gottlieb, S.A. Orszag, *Numerical Analysis of Spectral Methods: Theory and Applications*, CBMS-NSF Regional Conference Series in Applied Mathematics (SIAM, Philadelphia, 1977).

[10] J.S. Hesthaven, *Spectral Penalty Methods*, Appl. Numer. Math. **33**(2000), pp. 23-41.

[11] S. Karlin and W. Studden, *Tchebysheff Systems with Applications in Analysis and Statistics*, John Wiley (Interscience), New York, 1966.

[12] H.J. Landau, H. Widom, *Eigenvalue Distribution of Time and Frequency Limiting*, Journal of Mathematical Analysis and Applications, 77, 468-491(1980).

[13] D. Slepian, H.O. Pollak, *Prolate Spheroidal Wave Functions, Fourier Analysis, and Uncertainty - I* , The Bell System Technical Journal, January 1961.

[14] D. Slepian, *Prolate Spheroidal Wave Functions, Fourier Analysis, and Uncertainty - IV: Extensions to Many Dimensions, Generalized Prolate Spheroidal Wave Functions* , The Bell System Technical Journal, November 1964.

[15] H. Xiao, V. Rokhlin, N. Yarvin *Prolate Spheroidal Wave Functions, Quadrature, and Interpolation*, Research Report YALEU/DCS/RR-1199, 2000.